$K\alpha$ yields from Ti foils irradiated with ultrashort laser pulses

D. Riley,* J. J. Angulo-Gareta, F. Y. Khattak, and M. J. Lamb
School of Mathematics and Physics, Queen's University of Belfast, University Road, Belfast, BT7 1NN, Northern Ireland

P. S. Foster, E. J. Divall, C. J. Hooker, A. J. Langley, R. J. Clarke, and D. Neely
Central Laser Facility, CLRC Rutherford Appleton Laboratory, Chilton, Didcot, Oxon, OX11 0QX, United Kingdom
(Received 15 July 2004; published 14 January 2005)

We have studied the emission of $K\alpha$ radiation from Ti foils irradiated with ultrashort (45 fs) laser pulses. We utilized the fundamental (800 nm) light from a Ti:sapphire laser on bare foils and foils coated with a thin layer of parylene E (CH). The focusing was varied widely to give a range of intensities from approximately 10^{15}–10^{19} W cm^{-2}. Our results show a conversion efficiency of laser to $K\alpha$ energy of $\sim 10^{-4}$ at tight focus for both types of targets. In addition, the coated targets exhibited strong secondary peaks of conversion at large defocus, which we believe are due to modification of the extent of preformed plasma due to the dielectric nature of the plastic layer. This in turn affects the level of resonance absorption. A simple model of $K\alpha$ production predicts a much higher conversion than seen experimentally and possible reasons for this are discussed.

DOI: 10.1103/PhysRevE.71.016406 PACS number(s): 52.38.Ph, 52.38.Dx, 52.70.La

I. INTRODUCTION

Ultrashort bursts of $K\alpha$ emission from laser irradiated foils continue to be of widespread interest [1–8]. This is partly due to the potential of these sources to be generated on subpicosecond time scales [2]. The efficiency of such sources (typically 10^{-6}–10^{-3}) depends on the number and temperature of hot electrons generated at the front plasma surface by the presence of the incident laser beam. These factors in turn depend on parameters such as laser beam intensity, pulse length, pre-pulse level, wavelength, polarization, and angle of incidence. The experimental results and the Monte Carlo simulation reported by Eder *et al.* [3] demonstrate an optimum value for the Cu $K\alpha$ production as a function of the incident intensity. The theoretical model of Reich *et al.* [2] also suggests an optimal hot electron temperature for efficient generation of $K\alpha$ photons. In the latter, this is due to the depth of penetration of the electrons into a bulk target at high intensity. The $K\alpha$ photons generated deep within the foil are reabsorbed. In this paper we report on a study of $K\alpha$ yield from finite thickness Ti foils irradiated by short laser pulses with intensity ranging from 10^{15} W/cm^2 to 10^{19} W/cm^2. We do not observe a dip in the efficiency at tight focus but for CH coated targets we do observe evidence of broad peaks in efficiency at high values of beam defocus, indicative of some sort of optimization. We concluded in our earlier study that this was a result of the fact that at moderate intensities the response of the dielectric parylene coating to the low level pre-pulse was different than the response of bare Ti foils. This resulted in a shorter scale length generated at the plasma critical density. This in turn affected the efficiency of the resonance absorption process responsible for the generation of the fast electrons.

*Email address: d.riley@qub.ac.uk

II. EXPERIMENTAL SETUP

The experiments were carried out at the Rutherford Appleton Laboratory using the Ti:sapphire-based CPA system, ASTRA, delivering up to 150 mJ on target in infrared (800 nm), *p*-polarized pulses of 45(±5) fs duration. In addition to the pre-pulse activity at ~13 ns ahead of the main pulse and having a contrast of 10^{-7}, the main pulse is superimposed on a residual uncompressed CPA pedestal and ASE. The contrast of the residual uncompressed pedestal is measured to be 10^{-6} at 10 ps and rises to 10^{-4} at 1.5 ps ahead of the main pulse. The ASE starts 2 ns ahead of the main pulse and rises linearly from a background of 10^{-8} of the main pulse to a level of 10^{-6} in 1 ns and then stays constant until the main pulse arrives.

An $f/2.5$ off-axis gold-coated parabola was used to focus the IR beam at an angle of 10°–65° normal to the target plane. Focal spots at different positions were recorded in the low energy mode of the laser. The full width at half maximum (FWHM) of the focal spot at the best focus, shown in Fig. 1, was measured to be 3×3 μm. The FWHM contains about 55% of the total energy. The focal spot was varied by moving the parabola off the best focus position along the line of focus by a known amount with the help of a microcontroller, towards the target and away from the target (referred to as positive offset and negative offset, respectively). With the positive offset a convergent beam interacted with the target while in the case of negative offset the focus lay before the target and a divergent beam interacted with the target. As we moved off the best focus, the focal spot started breaking up into numerous hotspots and therefore the energy distribution in the focal spot changed. The energy on target was monitored for every shot with a calibrated fast diode and the maximum energy recorded on target was ~150 mJ. At the best focus, the intensity on target reached a maximum of $\sim 2\times 10^{19}$ W/cm^2.

Ti foils having a thickness of 12.5 μm, both bare and coated with 0.2 μm of CH, were used as the target. After

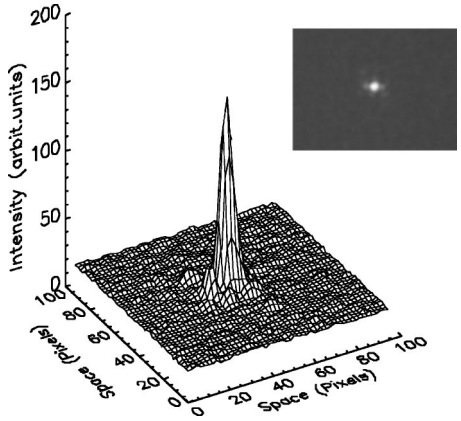

FIG. 1. Focal spot measured at low energy with a microscope objective. The central spot contains 55% of the energy and has a full width at half maximum of ~ 3 μm.

every shot, the foil was moved by 1 mm with an external computer controlled microdrive to get a fresh surface of the target for the laser interaction. In all cases, the beam was first tight focused on the foil, using a retro viewing system, that injected an alignment laser through the back of one of the dielectric mirrors and used the small amount of diffuse scatter from the target to monitor the position of best focus. After finding best focus, the parabola was moved to the desired offset position. A thin glass pellicle was used in front of the parabola to protect it from plasma debris. The time integrated $K\alpha$ line emission of titanium (4510.84 eV), was recorded with a Von Hamos spectrometer that consisted of an x-ray charge-coupled device (CCD) system coupled to a curved LiF (200) crystal with a reflectivity of 0.042 mRad [9]. The line of sight of the spectrometer (crystal center and the source position) made an angle of $\sim 48°$ with the horizontal plane.

III. RESULTS

In this section we present the data with some comments on the important features. Figure 2 shows the absolute $K\alpha$ yield for 800-nm irradiance on bare Ti targets at 45° and 20° angles of incidence as a function of focus position. Most data points are an average of three shots and the error bars in

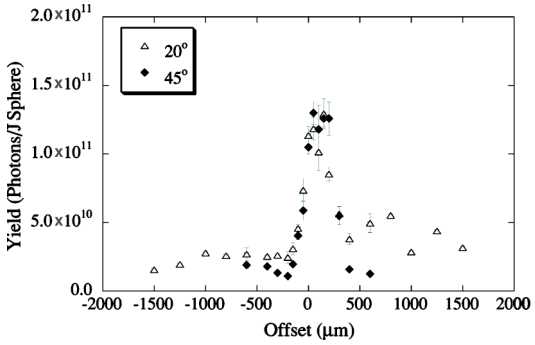

FIG. 2. $K\alpha$ yield for a bare Ti target as a function of offset. Negative offset means the focus is in front of the target.

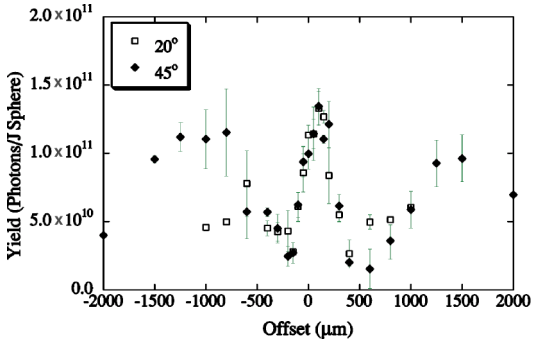

FIG. 3. $K\alpha$ yield for a coated Ti target as a function of offset.

yield are the statistical error. The error bar in the focal position is ± 20 μm. We can first notice that, for both angles of incidence there is a strong central peak of $\sim 1.5 \times 10^{11}$ photons/J/sphere, corresponding to a conversion efficiency of $\sim 10^{-4}$ from optical energy to $K\alpha$ energy. As we go towards negative offsets, the 20° data show a plateau with a gentle fall at very large offsets. For positive offsets, the yield seems to be higher. The 45° data do not extend as far but seem to systematically fall below the 20° data. In both cases, the central peak is offset from best focus by about 100 μm towards the positive. We think that this could be due to the fact that for positive offsets, the beam is converging as it interacts with the preformed plasma and refraction may lead to enhancement of the intensity at the critical surface. This is in contrast to the negative offset where refraction of a diverging beam may cause a lowering of the intensity at the critical surface. This effect is difficult to model in detail in a realistic way since it would require a multidimensional approach. Also the focal spot may have nonuniformities and at the high laser power (2.4 TW) there should be the possibility of relativistic self-focusing of the parts of or the whole beam to consider.

Figure 3 shows the $K\alpha$ yield from a Ti foil target coated with 200 nm of plastic irradiated at angles of 20° and 45°. As can be seen, this data also show a central peak for both cases of incidence with similar levels to the bare targets. In addition, the data for the 45° show strong and broad secondary peaks at larger offsets corresponding to $\sim 1 \times 10^{15}$ W cm^{-2} for positive offset and $\sim 2.5 \times 10^{15}$ for negative offset.

Broadly speaking the data are similar to data at 70-fs pulse duration published previously [9], where we explained this phenomenon in terms of absorption efficiency of the target. The general idea is that the CH coating is a dielectric and the ASE pre-lase must reach a higher intensity before a plasma forms—resulting in a shorter density scale length at the surface than for the bare Ti targets. This in turn gives better resonance absorption for 45° incidence. In this work we can proceed along a similar line but with some attempt to be quantitative regarding the yield. The longer scale lengths for the bare foils may explain why there is higher yield at the lower angle, except for small offsets. For the coated targets there is some evidence for the higher angle being more efficient away from best focus, as may be expected. At tight focus we do not expect a one-dimensional (1D) expansion and thus angle of incidence is less important as can be seen in Fig. 4 which shows an angle scan for best focus and both target types.

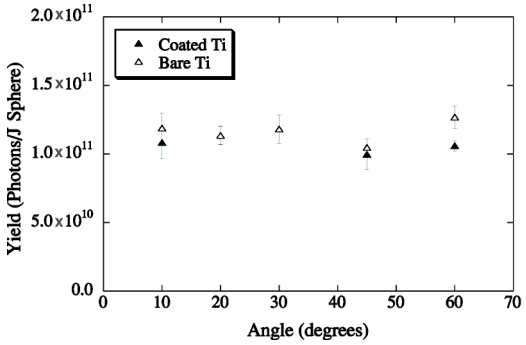

FIG. 4. $K\alpha$ yield for both bare and coated Ti targets as a function of angle of incidence at best focus.

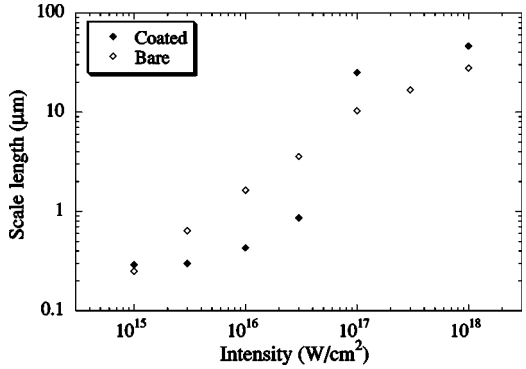

FIG. 5. Density scale length at the critical surface of the preformed plasma as calculated with the HYADES hydrodynamic code.

An important advantage of the coated targets is that with a high defocus we can have high efficiency but with a lower level of hard x-ray background. The $K\alpha$ signal sits on top of a uniform hard x-ray background. By use of filters and magnets we determined that this was principally caused by fluorescence from the crystal and substrate as hard x rays impinged on them. In terms of counts per pixel, this was at a higher count level than the $K\alpha$ signal itself. The signal was still easily measurable because of the uniformity of the background. Defining the noise level as the rms variation in background level over an area equivalent to the chip area on which the $K\alpha$ signal sat, we established a signal to noise ratio of 10 for tight focus, rising to ~50 at the secondary peaks of Fig. 3. Furthermore, if we look at the simulations of Reich *et al.* [2] it would seem also that at lower irradiance, the duration of the $K\alpha$ burst would be shorter due to the shorter stopping time of the fast electrons—this gives a further possible advantage of coated targets since a higher yield can be obtained for modest irradiance than for bare targets.

IV. SIMULATION AND DISCUSSION

A. Preformed plasma

Short pulse laser interaction with a solid target is a complex affair. A full simulation of the data presented here should in principle account for many things, including the generation of the preformed plasma, efficiency of absorption of laser light, generation of hot electrons with possibly more than one temperature—all in a multidimensional case with a nonuniform spot. The transport of the electrons through and around the target would then need to be modeled. Despite the advances in the subject area this is beyond our capabilities. However, it is still instructive to construct some simple models making some assumptions whose reasonableness can be tested or justified by reference to previous work.

The first stage of our simulation is to use the HYADES hydrodynamic code [10] to estimate the extent of the preformed plasma. We found that for moderate intensity cases the preformed plasma was shorter scale length for the coated targets since we ensured that plasma breakdown of the dielectric was not allowed to occur until a realistic energy density was reached (1 J cm^{-2}). For higher intensity, plasma was formed early in the ASE and the lower mass of the C and H ions meant the plasma expanded faster and gave a longer scale length [$L = n_c(\delta_n/\delta_x)^{-1}$] than the bare Ti case. Figure 5 shows our estimates up to an intensity of $\sim 10^{18}$ W cm^{-2}. At about this limit the scale length becomes larger than the experimental focal spot size and a 1D planar expansion is no longer valid. At high intensity, a purely spherical 1D expansion model, which assumes curved target surface with a radius of curvature equal to the spot size, predicts a scale length smaller than the focal spot size, indicating that in fact the limiting scale length is probably comparable to the focal spot size at high intensity cases.

B. Absorption and hot electron temperature

For cases at high defocus, where $L/D < 0.1$ (D = focal spot size), we can say that we have a planar situation on average and we have assumed that resonance absorption is the key absorption mechanism since we also generally have $L/\lambda > 0.1$. There is relatively simple model of the absorption due to this mechanism [11] and some theoretical as well as experimental estimates of the hot electron temperature in the appropriate intensity regime [2,12,13]. At higher irradiance, a planar model is not appropriate and the hot electron generation is more likely to be due to ponderomotive acceleration for which the scaling of hot electron temperature is available [12,14].

Work by Snavely *et al.*, Pisani *et al.*, and Wharton *et al.* [15–17] has covered the range from $\sim 10^{18}$–3×10^{20} W cm^{-2} and we have plotted their results for absorption fraction in Fig. 6(a), along with a power law fit to the absorption as a function of irradiance. We have used this fit to estimate absorption at the high intensity regime down to $\sim 10^{17}$ W cm^{-2} where resonance absorption is predicted to be appropriate and dominant. The effect on the assumed absorption is seen in Fig. 6(b). Although the resonance absorption levels from the simple theory look high, there is experimental evidence [18,19] for high absorption in the correct circumstances and we leave the model as it stands for now.

As a check, we ran the code MEDUSA [20], which allows us to set up an initial preformed plasma and looked at how much inverse bremsstrahlung absorption is predicted for each case. The code included the strong field correction and the level of absorption was only a few percent. Thus we have assumed in our modeling that inverse bremsstrahlung is relatively unimportant.

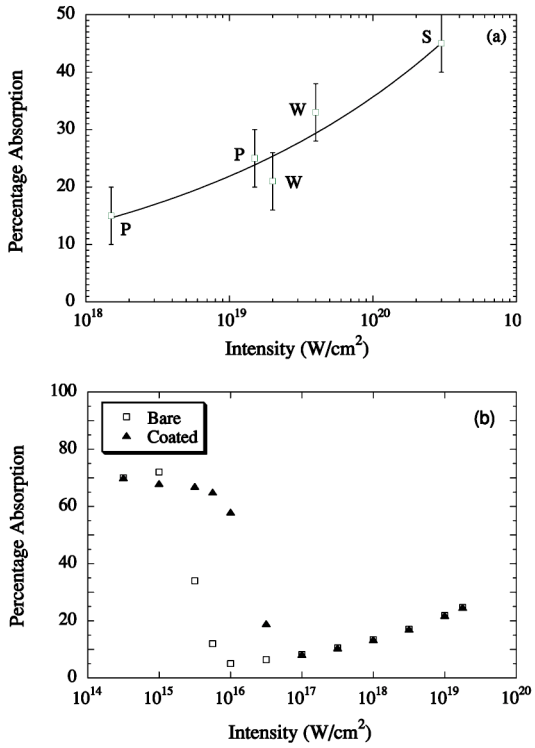

FIG. 6. (a) Absorption results from other authors, *P*=Pisani *et al.*, *W*=Wharton *et al.*, and *S*=Snavely *et al.* The power law fitted scales absorption as $\sim I^{0.2}$. (b) Assumed absorption used in the modeling below, as a function of irradiance for both target types.

We consider in our simulations below three scaling laws for hot electron temperature. The first comes from PIC simulations by Reich *et al.* [2] and has $T_{\mathrm{hot}}=110(I_{17})^{1/2}$ keV, where I_{17} means the intensity in units of 10^{17} W cm^{-2}. The second is experimental data reported by Nishimura *et al.* [13] and has $T_{\mathrm{hot}}=29(I_{17})^{0.74}$ keV. These two are options for the lower intensity regime where resonance absorption is the main mechanism. Finally, we use the ponderomotive heating law [12,14] which has $T_{\mathrm{hot}}=mc^2[(1+a_0{}^2)^{1/2}-1]$, where a_0 is given by $(I\lambda^2/1.4\times10^{18}$ W cm^{-2} μm$^2)^{1/2}$. This latter is, of course, more likely to be applicable at higher intensity.

C. $K\alpha$ generation

After considering the possible absorption fractions and hot electron scaling we consider the manner in which $\widetilde{K}\alpha$ photons are generated by the fast electrons. We adopt two distinct approaches to explore the issues and concentrate initially on the bare targets.

1. Cross-section model

In our first approach a numerical model is used to split the foil into 100 layers. The slowing of the electrons through each layer is calculated with a simple Bethe-Bloch model [21]. For higher irradiances this is not in fact a very large effect for the foils used. The cross section for *K*-shell ionization as a function of energy, including relativistic correction [22], is used with the fluorescence yield [23] of Ti ($\sim$0.19) to calculate the emission seen from each layer. The reabsorption is accounted for using the depth of each layer and the known opacity of cold solid Ti at the $K\alpha$ photon energy. This model assumes that any electron leaving the foil is lost and plays no further role. Figure 7 shows the predicted yield including the variation of absorption with intensity, but, for now, using each temperature scaling law in turn for all intensities. We can see that contrary to our experimental results, the yield is predicted to fall towards the highest intensity in all three cases. At modest intensity, there is an optimum with different irradiances depending on the scaling law used. Reich *et al.* [2] report a similar optimum, although, as mentioned above, in their case it is due to reabsorption. For our thin foil case, it is because at higher intensity there are fewer hot electrons and they mostly escape the foil and at low intensity many of the electrons are not energetic enough to ionize Ti. It is clear that recirculation of electrons that leave the rear of the foil must take place. This is in accordance with the experiments of Malka *et al.* [24] and Malka and Miquel [25], where less than 1% of laser energy is estimated to escape from the targets as fast electrons.

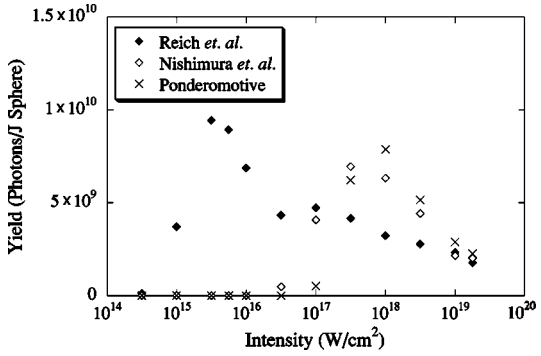

FIG. 7. Yield for bare targets given by simple cross-section model that assumes electrons only pass once through the foil. Three separate models of hot electron temperature are used.

2. Empirical model

In this approach, we use a method derived from that of Reich *et al.* [2]. We assume the fast electrons have a quasi-Maxwellian distribution and stream into the foil. Using the empirical data of Green and Cosslet [26] we estimate that electrons of energy E (keV) create $\widetilde{K}\alpha$ photons according to

$$N_{\mathrm{gen}}(E) = 4\times10^{-5}(E-E_0)^{1.63},$$

where E_0 is the *K*-shell ionization energy. Since this model does not follow the trajectory of the electrons we have corrected for reabsorption by assuming the photons originate on average from the center of the foil—this is not a large effect for our relatively thin foil.

This model is really best suited to a bulk target and in our case we need to make the implicit assumption that electrons that emerge from the rear of the target are reflected back into the target by space charge effects. Again this view is supported to some degree by the observation [24,25] that only a small fraction of laser energy escapes from a foil irradiated by a high power ultrashort pulse laser in the form of fast

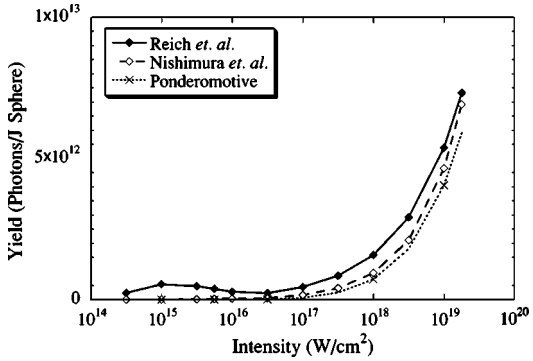

FIG. 8. Yield for bare targets using a simple model for $K\alpha$ yield as a function of electron energy assuming all electrons pass back and forth through the foil until they lose their energy. Again, three separate models of hot electron temperature are used.

electrons. The predicted emission of $K\alpha$ photons from the bare Ti foil, when combined with assumed absorptions, is shown in Fig. 8—again for all three assumptions about temperature scaling. As can be seen, the predicted emission rises towards tight focus as seen experimentally but is more than an order of magnitude greater than observed. We know that the electrons will move out of the focal spot volume as it has been observed that the *K*-alpha source size can be several times the laser spot size [3,27]. However, this does not mean that they escape from the foil. Our data were not spatially resolved and any emission from a reasonably large area would be collected. The predicted yield at low irradiance/high defocus offset is much more in line with experiment than the simple cross-section model. We emphasize again that thus far this model assumes that all fast electrons enter the cold foil and are completely recirculated into the target as they emerge from the rear. This and other assumptions are discussed in the next subsection.

D. Discussion

The empirical model described above is based on what we consider to be fairly sound estimates of absorption and hot electron temperature based on the previous experience of other researchers. The conversion of fast electrons to $K\alpha$ photons is based on experimental data. The assumption that little energy is lost to escaping electrons seems to be backed up by experimental observations. However, the experimental yield is a factor of $\sim$50 less than the simulations at tight focus. This is perhaps not such a surprise as the model we have used is quite simplistic and indeed Reich *et al.* also generate yields well in excess of the experimental data to which they compare their results [6]. On the other hand, the cross-section model is also based on similarly straightforward ideas and also does not match experiment. In the latter it is clear that a weakness of the model is that it allows many of the electrons to escape the rear of the foil contrary to experimental experience. For the empirical model we can point to two areas of weakness.

First, it is assumed that when the electrons are recirculated they effectively just switch direction without loss of energy. For the tight focus case our empirical model required this to happen many times for the fast electrons. In fact it is likely that electrons leaving the cold foil will pull ions with them, thus transferring energy out of the electron beam. The behavior in the extended preformed plasma may well be different to that at the sharp boundary on the rear surface but both need to be considered as potential energy losses.

Second, and perhaps more obviously, we are assuming in our calculations that all electrons will enter the cold part of the foil despite the potentially important role of electric field inhibition [28,29]. Indeed, we can note that if we consider a simple model of a capacitor, where the charge separation is between the critical density surface and the solid foil (about 10–20μm in a 1D planar simulation), then moving $\sim$2% of the charge generated at tight focus ($T\sim$1.5 MeV with 25% absorption of laser light) creates a potential of $\sim$8 MV in the absence of return current. For a Maxwellian at T_{hot} $\sim$1.5 MeV only $\sim$2% of electrons have more than this energy, so that there is scope for this mechanism to inhibit electron penetration. In reality, such a large field would drive a substantial cold return current to balance this and the penetration of the fast electrons into a solid would depend on the metallic/dielectric nature of the cold foil [16]. Although Ti is a metal, its cold conductivity is, for example, a factor of 15 less than for Al and so there may be stronger inhibition than for Al targets. With such a short pulse duration, there is clearly some scope for further work looking at the detailed modeling of electron transport in this particular experimental arrangement.

The current capability of our own modelling is not sufficient to carry out this work as there are details of the geometry of the laser interaction and fast electron generation to account for as well as the generation of return current and transport of the fast electrons in the solid. Nevertheless, we can try to think about our disagreement between experiment and modeling by looking at the scaling for some parameters that may affect the effectiveness of fast electron penetration of the foil.

First, on the issue of inhibition due to electric field generation, we note that, if the hot electron temperature scales as $\sim I^{1/2}$ at high intensity and the area of the focal spot varies inversely with I, as it does for fixed laser energy, then for a given absorption level, the number of fast electrons per unit area (and thus current) required to penetrate into the target scales as $\sim I^{1/2}$. The areal charge density separated in turn affect the electric field generated.

Second, looking at a different point of view, we require the electrons to penetrate the foil, but for ponderomotive heating with a small focal spot size, a substantial number of electrons may be expelled laterally from the focal region rather than forward into the foil. Such electrons may give energy to the expansion of the plume but might not enter the cold solid. The degree to which this occurs, should be governed by the ratio of focal spot perimeter to area which varies as $I^{1/2}$.

Finally, we can note that for the fast electrons the foil is much less than the Bethe-Bloch stopping distance and that Feather's law [21] gives a linear relationship between ultimate range and electron energy. Thus, to an approximate degree, the loss rate varies as T_{hot}^{-1} and thus $I^{-1/2}$. Therefore our empirical model assumes that fast electrons make a num-

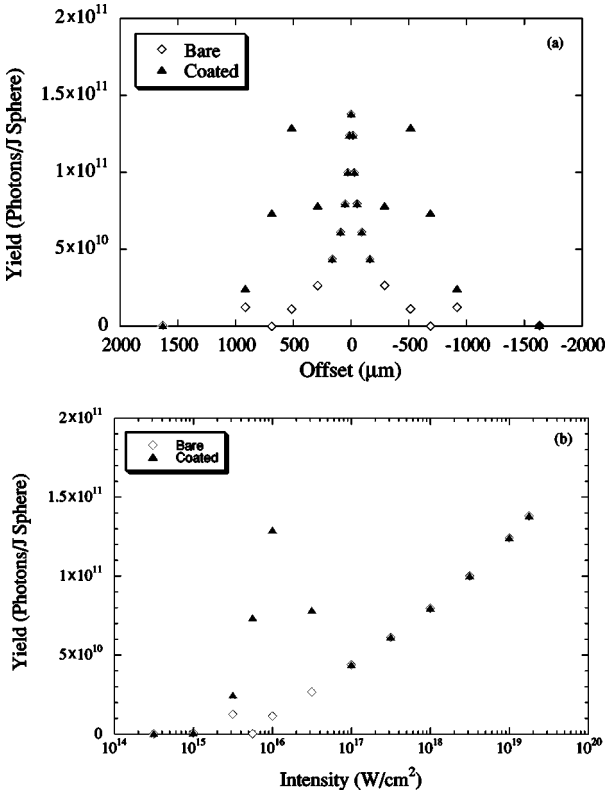

FIG. 9. Yield as a function of (a) offset and (b) corresponding intensity for a composite model using the Nishimura *et al.* scaling of hot electron temperature at low intensity and the ponderomotive heating model at high intensity. The absorption is given by Fig. 6(b) and an *ad hoc* loss factor is added as discussed in the text.

ber of "passes" through the foil that varies as energy and thus, on average, as $\sim I^{1/2}$. For each of these hypothetical passes we ought to be accounting for some energy loss.

Taking these points into consideration we wish then to make an *ad hoc* hypothesis that there is a "correction" factor to be applied to our model to account for the inefficiencies described and that it has a value of ~ 50 at the highest intensity and thereafter scales as $I^{1/2}$. Figure 9 shows the results of applying such a "correction" factor to simulations that use the experimentally derived Nishimura *et al.* hot electron temperature scaling at lower intensity when resonance absorption is thought to be dominant and the ponderomotive heating scaling otherwise. We can see that the general shape of the experimental data is now reasonably well reproduced. The central peak height is of course set to match experiment by the choice of maximum "correction" factor, but the secondary peaks for the coated targets are roughly the correct height compared to the central peak and are not so evident for the bare targets.

The results of Fig. 9 are quite pleasing when compared to the experimental data presented—there is a difference in the offset of the secondary peak for the coated targets but the overall picture is reproduced. However, it is important to note some other scaling laws for fast electron temperature tend to have a higher temperature at lower intensities and would give, in Fig. 9, a secondary peak much in excess of the central peak and above what experiment tells us. Thus we need to exercise caution before being too satisfied with Fig. 9. We could in principle approach the problem from another point of view and use the cross-section model with some factor used to account for the return of electrons to the foil once they pass through the rear surface as well as the efficiency with which they penetrate the cold foil initially. However, this would again be an *ad hoc* correction. We must also note that, apart from the fast electron transport issues and the wide variation fast electron temperature predicted by different models at modest irradiances (below $\sim 10^{17}$ W cm^{-2}) more than one fast electron temperature may be present in the plasma.

In summary, we have shown that relatively high $K\alpha$ production has been possible with the laser energy at the fundamental frequency from an ultrashort pulse (45 fs) Ti:sapphire laser. We have shown that the efficiency can be experimentally manipulated to be high at modest intensity (and lower hard x-ray background) by the use of coatings to modify the preformed plasma scale length. Finally, we show that a simple model overestimates the experimental yield (especially at high intensity) because it neglects some factors that may affect efficiency with which the fast electrons are coupled to the foil. By making some assumptions about how these factors vary with intensity it has been possible to reproduce the experimental data in broad outline. By taking more data with a range of target thickness, we may be able in the future to deduce more about the mechanisms governing how efficiently we can generate $K\alpha$ sources.

ACKNOWLEDGMENTS

We would like to thank the target preparation staff of the Rutherford Appleton Laboratory. This work was supported by EPSRC Grant No. GR/R09572/01.

[1] A. Rousse *et al.*, Phys. Rev. E **50**, 2200 (1994).
[2] Ch. Reich *et al.*, Phys. Rev. Lett. **84**, 4846 (2000).
[3] C. D. Eder *et al.*, Appl. Phys. B: Lasers Opt. **70**, 211 (2000).
[4] K. B. Wharton *et al.*, Phys. Rev. E **64**, 025401 (2001).
[5] T. Feurer *et al.*, Phys. Rev. E **65**, 016412 (2001).
[6] D. Salzmann *et al.*, Phys. Rev. E **65**, 036402 (2002).
[7] Ch. Ziener *et al.*, Phys. Rev. E **65**, 066411 (2002).
[8] F. Ewald *et al.*, Europhys. Lett. **60**, 710 (2002).
[9] F. Y. Khattak *et al.*, J. Phys. D **36**, 2372 (2003).
[10] J. T. Larsen and S. M. Lane, J. Quant. Spectrosc. Radiat. Transf. **51**, 179 (1994).
[11] W. L. Kruer, *Introduction to Laser Plasma Interactions* (Addison-Wesley, Reading, MA, 1988).
[12] F. Amiranoff, Meas. Sci. Technol. **12**, 1795 (2001).
[13] H. Nishimura *et al.*, J. Quant. Spectrosc. Radiat. Transf. **81**, 327 (2003).

[14] S. C. Wilks *et al.*, Phys. Rev. Lett. **69**, 1383 (1992).
[15] R. A. Snavely *et al.*, Phys. Rev. Lett. **85**, 2945 (2000).
[16] F. Pisani *et al.*, Phys. Rev. E **62**, R5927 (2000).
[17] K. B. Wharton *et al.*, Phys. Rev. Lett. **81**, 822 (1998).
[18] U. Teubner *et al.*, Phys. Rev. E **54**, 4167 (1996).
[19] Q. L. Dong, J. Zhang, and H. Teng, Phys. Rev. E **64**, 026411 (2001).
[20] J. P. Christiansen, D. E. T. F. Ashby, and K. V. Roberts, Comput. Phys. Commun. **7**, 271 (1974).
[21] W. E. Burcham, *Elements of Nuclear Physics* (Longman, London and New York, 1979).
[22] C. A. Quarles, Phys. Rev. A **13**, 1278 (1976).
[23] *X-ray Data Booklet* (Centre for X-ray Optics, LBNL, 1986).
[24] G. Malka *et al.*, Phys. Rev. E **66**, 066402 (2002).
[25] G. Malka and J. L. Miquel, Phys. Rev. Lett. **77**, 76 (1996).
[26] M. Green and V. E. Cosslet, J. Phys. D **1**, 425 (1968).
[27] Ch. Reich *et al.*, Phys. Rev. E **68**, 056408 (2003).
[28] A. R. Bell *et al.*, Plasma Phys. Controlled Fusion **39**, 653 (1997).
[29] J. Davies, Phys. Rev. E **68**, 056404 (2003); **69**, 065402 (2004).